ELSEVIER

Scientia Horticulturae 69 (1997) 169–179

SCIENTIA HORTICULTURÆ

Freezing effects in fruit tissue of kiwifruit observed by magnetic resonance imaging

W.L. Kerr [a], C.J. Clark [b,*], M.J. McCarthy [c], J.S. de Ropp [d]

[a] *Department of Food Science and Technology, University of Georgia, Athens, GA 30602, USA*
[b] *HortResearch, Palmerston North Research Centre, Private Bag 11030, Palmerston North, New Zealand*
[c] *Department of Food Science and Technology, University of California, Davis, CA 95616, USA*
[d] *NMR Facility, University of California, Davis, CA 95616, USA*

Accepted 8 January 1997

Abstract

Formation of ice, and the dynamics of freezing in immature kiwifruit (*Actinidia deliciosa* var. *deliciosa* cv. 'Hayward'; 4.7–6.8% total soluble solids) was observed by NMR imaging. Freezing was induced by subjecting detached fruit to circulating air at −40°C and monitored by spin-echo imaging. Comparisons were also made between measurements of spin-spin (T_2) relaxation and the self-diffusion coefficient (D) in fresh and frozen-thawed samples. Formation of ice was visualised by loss of signal in affected areas of the fruit, freezing commencing at the epidermis and gradually progressing towards the core. Freezing tended to be asymmetric (in some fruit ice tended to move more rapidly through the core than through other tissues) and governed by the air-flow conditions (regions most directly exposed to the air-flow froze preferentially). T_2 relaxation was faster, and D coefficients greater in frozen-thawed fruit compared with fresh fruit. The significant decrease in T_2 relaxation following freezing has implications for design of on-line sensors distinguishing between damaged and undamaged fruit. © 1997 Elsevier Science B.V.

Keywords: *Actinidia*; Freezing; Frost injury; Fruit; Kiwifruit; Magnetic resonance imaging; Non-destructive analysis

1. Introduction

Kiwifruit (*Actinidia deliciosa* [A. Chev.] C.F. Liang et A.R. Ferguson var. *deliciosa*) typically require 25 weeks from anthesis to reach physiological maturity—the earliest time at which the fruit can be removed from the vine yet still continue to ripen

* Corresponding author. Tel. 64-6-351-7096; Fax, 64-6-354-6731; E-mail, ClarkC@hort.cri.nz.

PII S0304-4238(97)00006-X

satisfactorily (Beever and Hopkirk, 1990). This long growing season increases the likelihood that both mature and immature fruit may be exposed to, and damaged by, autumn frosts (Young, 1987; Testolin and Costa, 1995). Except in circumstances in which fruit are extensively damaged by frost and a bluish discolouration symptomatic of water-soaked flesh is evident under the skin, external symptoms associated with lesser degrees of injury are practically impossible to detect visually (MacRae and Aldridge, 1984). Frost-damaged fruit subsequently develop abnormal and undesirable quality characteristics during storage if not removed at harvest (Pyke et al., 1985). This lead to evaluation of non-destructive methods such as ultrasonics, light scattering and chlorophyll fluorescence, as possible sensors for discriminating between frost-affected and non-affected fruit, none of which proved successful (Ballagh et al., 1984). Nuclear magnetic resonance (NMR) imaging, which was not widely available at the time of Ballagh's study, was not included in this evaluation.

In recent years, NMR techniques have been used to monitor changes in foods at harvest, during postharvest storage, and during processing (McCarthy, 1994). For example, Chen et al. (1995) developed an on-line NMR sensor to evaluate maturity of avocados and prunes, while McCarthy et al. (1995) investigated the bruising process in apple. Applications of NMR related to changes following freezing of fruit are rare, but include Duce et al. (1992), who found qualitative changes in NMR images of courgette before and after freeze-thawing, and Gamble (1994), who noted changes in the exchange properties of aqueous protons at discrete locations within the fruit, after freezing and thawing fresh blueberries.

The purpose of this study was to determine if NMR imaging could be used to monitor freezing as fruit were gradually cooled to subzero temperatures. In addition, we wished to establish whether freeze damage could be detected and related to changes in various properties measured by NMR. In this study, we monitored changes occurring under laboratory conditions in order to determine those properties and instrumental conditions which would be pertinent. If proven feasible, the goal for the future would be to develop NMR techniques for non-destructive detection of frost-injured fruit. Particular properties investigated included: structural changes as imaged by NMR; changes in NMR relaxation parameters; and changes in diffusion of water molecules.

2. Materials and methods

2.1. Plant material

Fruit for imaging were obtained from a research orchard located near Hamilton, New Zealand, from vines (cv. 'Hayward') grafted to 1-year-old seedling rootstock in 1982. Samples, each comprising ten fruit, were picked on three occasions around the time of commercial harvest; 1, 15 and 25 May 1995. The soluble solids content of companion samples at these times was 4.7, 5.5 and 6.8%, respectively (commercial harvesting commences once fruit have reached 6.2% soluble solids). Fruit were individually nested in shredded paper inside a polystyrene container, which was then firmly sealed and dispatched by airfreight to Davis, California, within 2 h of picking. The container reached its destination within 4 days. The temperature profile of the fruit while in transit

was not recorded; however, all fruit arrived undamaged and apparently unaffected by the shipping process as determined by visual inspection. No frosts were recorded during the period 1–25 May at the research orchard. Samples used for imaging can therefore be regarded as being 'typical' for their stage of development. Experiments were also run on kiwifruit obtained from the Davis area. These were mature, eating-ripe fruit with a soluble solids content of 12.5%.

2.2. *Magnetic resonance imaging during freezing*

Images were collected on a GE-NMR Omega spectrometer operating at 7.05 Tesla. Images were acquired using a spin-echo pulse sequence (Edelstein et al., 1980) and a slice thickness of 4 mm. Datasets were collected as 128×256 points and zero-filled to 256×256 points.

In preliminary experiments to observe the freezing process in kiwifruit, single fruits were suspended by their stems in an insulated cabinet, $40 \times 40 \times 30\,cm^3$. Cold air at $-40°C$ was circulated in the cabinet at an entrance velocity of $5\,m\,s^{-1}$. Fruit were removed at approximately 15 min intervals and imaged immediately.

To observe the freezing process in situ, a 10-cm-diameter PVC pipe was centred through the bore of the magnet. Single fruit were placed in the tube, and within the confines of a 'birdcage' imaging coil. Cold air at $-40°C$ was directed through the tube while the fruit were being imaged, the long axis of the kiwifruit being oriented parallel to the air flow. A 70-mm field-of-view (270 μm resolution) centred on a median transverse slice through the fruit was used for obtaining images at successive time intervals. The total time for acquisition of spin-echo images was 4.25 min. To speed data acquisition FLASH images (Haase et al., 1986) were collected with 100 ms recycle times, reducing the overall acquisition time to 25 s. Images of the freezing process obtained by either spin-echo or FLASH pulse sequences revealed no significant differences.

2.3. T_2 *measurements in fresh versus frozen-thawed fruit*

In subsequent experiments, several of the fully frozen fruit were allowed to thaw at room temperature. One fresh and one frozen-thawed fruit were placed side-by-side in the imaging coil. Images were collected as 100 mm transverse slices, giving simultaneous views of the fresh and thawed fruit. To enable a spatially resolved analysis of the spin-spin relaxation parameter, T_2, the echo time (T_E) in the spin-echo pulse sequence was varied between 16 and 500 ms. The maximum amplitude of the spin echo is given by (Callaghan, 1991):

$$M_y = M_0\{1 - 2\exp[-(T_R - T_E/2)/T_1] + \exp(-T_R/T_1)\} * \exp(-T_E/T_2) \quad (1)$$

where T_R is the time between repetitions of the pulse sequence, M_0 is the initial signal intensity following excitation, and M_y, the signal intensity at time T_E. By setting T_R (2500 ms) much larger than T_E and T_2, Eq. (1) reduces to

$$M_y = K\exp(-T_E/T_2) \quad (2)$$

where K is a constant proportional to the density of protons. Thus, a semi-log plot of signal intensity versus T_E at any given point in the image should give a straight line with slope $-1/T_2$.

2.4. Diffusion measurements in fresh versus frozen-thawed fruit

In other experiments, diffusion-weighted images were obtained as follows. It can be shown, that for a pulsed-gradient-spin-echo sequence (Callaghan, 1991) the echo amplitude obtained with a gradient, $S(g)$, compared with that with zero gradient, $S(0)$ is:

$$S(g)/S(0) = \exp\left[-D\gamma^2 g^2 \delta^2 (\Delta - \delta/3)\right] \quad (3)$$

where D is the self-diffusion coefficient of water; γ, the gyromagnetic ratio for protons; g, the gradient strength; δ, the time over which the gradient is applied; Δ, the diffusion delay time. By varying Δ at constant γ, δ, and g, the self-diffusion coefficient can be determined from a semi-log plot of $S(g)/S(0)$ versus $\gamma^2 g^2 \delta^2 (\Delta - \delta/3)$. Alternatively, at constant γ, g, δ, and Δ, simultaneous imaging of fresh and frozen-thawed kiwifruit will show decreased signal intensity where diffusion of water is most rapid, particularly at longer diffusion times. In these experiments a gradient (g) of 2.5 G cm^{-1} was applied for $\delta = 15$ ms, while Δ was varied from 70 to 210 ms.

2.5. NMR spectra from fresh versus frozen-thawed fruit

Spectra of juice from fresh and frozen-thawed fruit were compared using high-resolution NMR spectroscopy. One-dimensional proton NMR spectra of solutions contained in 5 mm tubes were obtained on a GE-NMR spectrometer operating at a field strength of 11.75 Tesla. Datasets were collected with 16 384 points over a 6 kHz bandwidth. A 90° pulse was used in conjunction with a 3.7 s recycle time. A 1 s selective pulse was used to saturate the water signal prior to the 90° pulse. Thirty-two scans were collected for each spectrum and the data Fourier transformed without apodization. Peak shifts were referenced to water which in turn had been calibrated to internal 2,2-dimethyl-2-silapentane-5-sulphonate as 0.0 ppm.

3. Results

3.1. Images during freezing

Fig. 1 shows images of kiwifruit exposed to circulating air (−40°C) at increasingly longer periods of time. Images at zero time show much of the structural morphology of the fruit, including the core, inner pericarp (seed-bearing tissues) and outer pericarp (flesh). Brighter regions correspond to higher signal intensity and thus can be associated with greater density of liquid water or regions with larger T_2 relaxation times. The locules in the inner pericarp which contain the seeds (but not the seeds themselves), show the greatest initial intensity. Formation of ice is seen as a marked decrease in

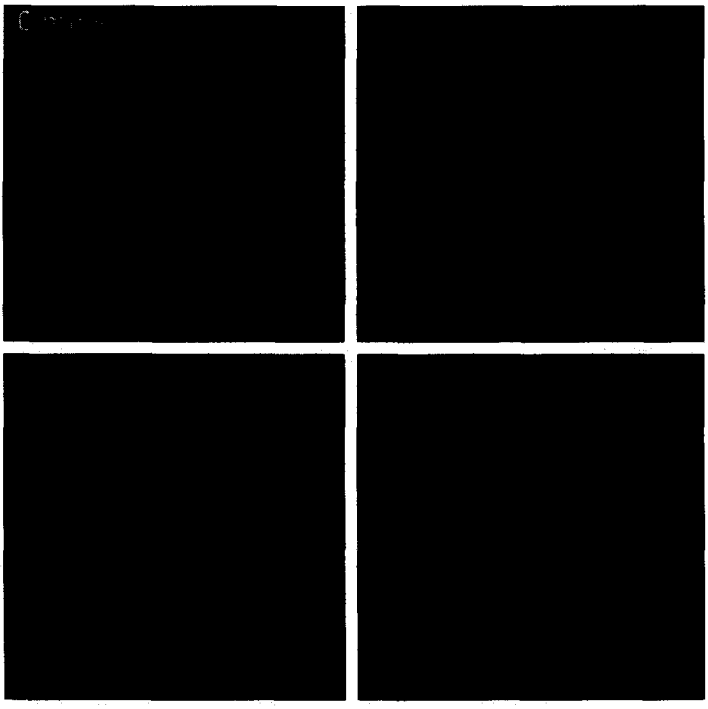

Fig. 1. Progression of freezing in a median longitudinal slice of kiwifruit monitored by spin-echo imaging (resolution 390 μm; $T_R = 1000$ ms, $T_E = 25$ ms) at the indicated time points. Freezing was induced by suspending fruit in flowing air at −40°C in a chamber prior to placing samples in the magnet.

signal intensity. Epidermal layers adjacent to the fruit surface froze within 15 min exposure to the cold air, with freezing commencing from the outer regions of the fruit and progressing towards the core.

Where samples were frozen within the magnet (data not shown), ice formation occurred preferentially in those areas directly facing the flow of cold air. In most cases, ice formed throughout the entire sample after approximately 45 min.

3.2. Structural changes after thawing

Morphological structures were clearly visible where images of both fresh and frozen-thawed samples (3-h thawing) were obtained simultaneously (Fig. 2). Several distinguishing observations were made in most of these comparisons. Once thawed, the samples became very flaccid and deformed easily by pressure from the weight of the fruit itself at the point of contact with external surfaces, and slight mechanical compression during shifting. As a consequence, the oval appearance of transverse image sections assumed more irregular geometries. One such indentation can be seen on the left-hand-side of the thawed fruit in Fig. 2. In other cases (data not shown), the regular pattern of the seed structure was frequently disrupted after freeze-thawing resulting in a more random distribution of the seeds.

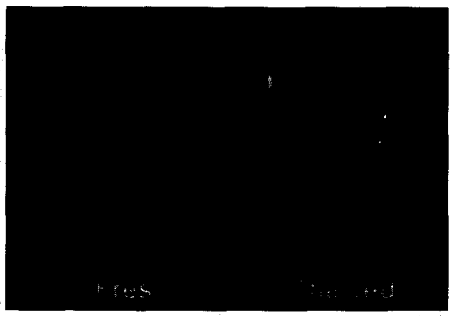

Fig. 2. A transverse slice through a fresh (left) and frozen-thawed kiwifruit (right) obtained simultaneously by spin-echo imaging (resolution 390 μm; $T_R = 1000$ ms, $T_E = 19$ ms). Indentations such as that observed on the left-hand-side of the thawed fruit occurred readily at the point of contact between the flaccid flesh and external surfaces, and by slight mechanical compression during positioning.

3.3. Changes in T_2 relaxation after freeze-thawing

T_2 weighted images are shown at echo times of 16, 90 and 300 ms (Fig. 3). The thawed, deformed, kiwifruit (on the right) is visible at 16 ms. At 300 ms, the inner pericarp of the fresh fruit is still visible, while the same tissue in the thawed sample is not. This suggests that T_2 relaxation is faster in the thawed fruit. This was confirmed by T_2 measurements of the bulk water resonance on nine separate samples of fresh and thawed fruit using a Carr-Purcell-Meiboom-Gill (CPMG) pulse sequence. The average T_2 for fresh fruit was 312(42) ms (standard deviation in parentheses) compared with 208(36) ms for the thawed fruit: a difference significant at $P < 0.01$.

3.4. Changes in diffusion after freeze-thawing

Diffusion-weighted images of fresh and frozen-thawed kiwifruit were obtained at diffusion times (Δ) varying from 70 to 210 ms (Fig. 4). At longer times, signal intensity

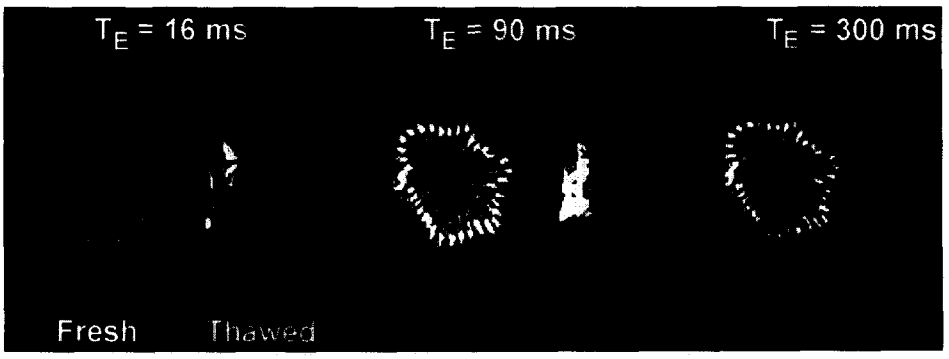

Fig. 3. T_2-weighted spin-echo images (resolution 390 μm) of fresh and frozen-thawed kiwifruit acquired with varying echo time delays (T_E) and $T_R = 2500$ ms.

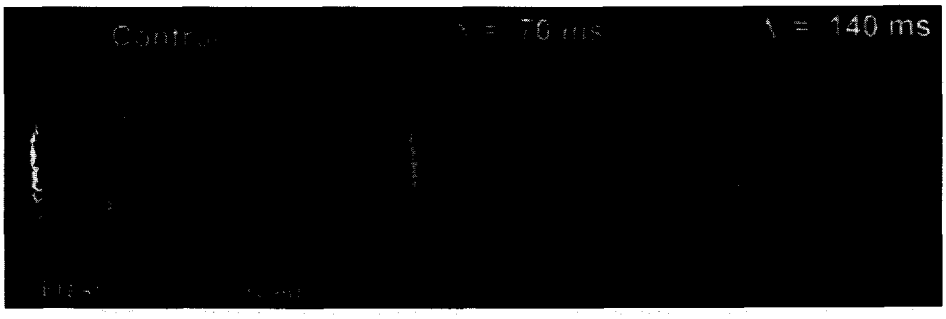

Fig. 4. Diffusion-weighted images (resolution 390 μm) of fresh and frozen-thawed kiwifruit acquired at different diffusion delay times (Δ) and a diffusion gradient of 2.5 G cm^{-1}. In the control (left-hand panel) Δ = 70 ms, and the diffusion gradient = 0. Image contrast in the control thus contains only static information about proton distribution, as opposed to the other two panels in which image contrast relates to dynamic properties (see text for further details).

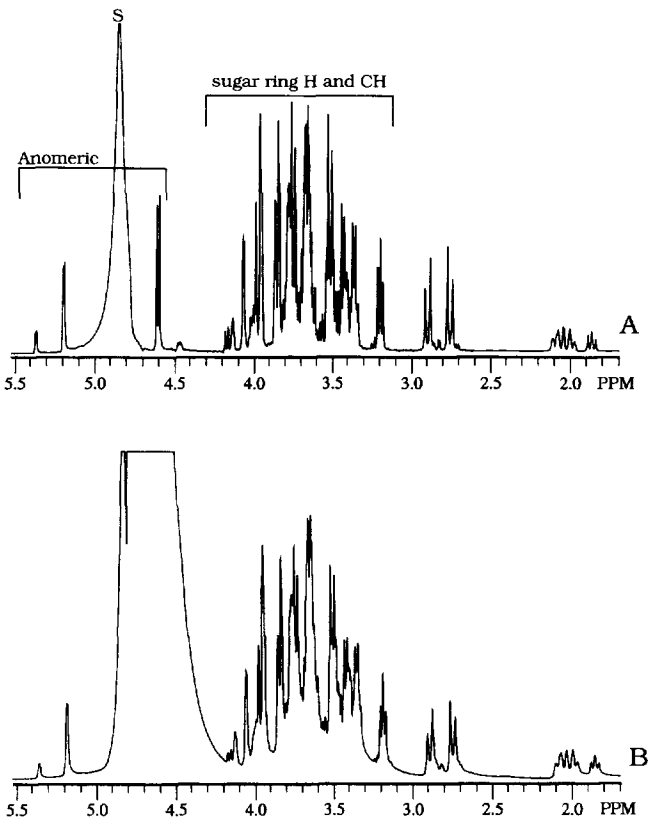

Fig. 5. 500 MHz proton NMR spectra of juice from fresh (A) and frozen-thawed (B) kiwifruit. Peak assignments are on trace (A): peak S is bulk water.

diminished most in the freeze-thawed fruit. At $\Delta = 140$ ms, signal had been lost from all regions of the thawed fruit, while signal could still be detected in the fresh fruit, and the inner pericarp in particular. This indicates that diffusion was more rapid in the freeze-thawed samples.

3.5. NMR spectra of fresh versus frozen-thawed fruit

Plots of the NMR chemical spectra of juice from fresh and freeze-thawed kiwifruit showed chemical shifts for those components readily dispersed in the aqueous phase (Fig. 5). The large peak around 4.8 ppm is due to water, while the peaks downfield of 3.0 ppm can be associated with low molecular weight sugars (such as glucose, fructose and sucrose). The peaks upfield of 3.0 ppm were not assigned. The narrow line widths across the whole spectrum argue against the presence of high molecular weight species in the aqueous phase. Comparison of spectral peaks in the two types of sample shows little, if any difference, in solution composition.

4. Discussion

Formation of ice, and the nature and dynamics of the freezing process in kiwifruit was readily visualised using NMR imaging. The signal observed in these experiments is proportional to the density of the remaining mobile protons, since the relaxation processes for the protons associated with ice (and solids generally) are so rapid that they do not effectively contribute (Kerr et al., 1996). How ice forms in the fruit depends on its geometry and composition, as well as the heat transfer characteristics of the environment and the presence of ice-nucleating agents. The images showed freezing to be asymmetric and governed by the air-flow conditions. When air-flow was directed from beneath the fruit (as in the freezing chamber), or at the point of contact with the flow-stream within the confines of the magnet, those regions most directly exposed to cold air displayed greater extents of freezing. Moreover, certain regions of the fruit appeared more susceptible to freezing than others. In some samples, for example, ice advanced more rapidly through the core. This may be due to breaks in the skin or at the picking scar, which allow water frozen at the surface to propagate through the stem (peduncle) and into the fruit, rather than relative differences in freezing point depression. Total soluble sugars in the three tissue types (core, inner and outer pericarp), and in basal, median and distal regions of the fruit are similar, at least until the time of commercial harvest: thereafter the concentration in the core tends to be higher than that in the other two tissues (C.J. Clark, unpublished data, 1996). Core tissue would thus be expected to be the last to freeze, rather than the first, if based on compositional arguments alone.

The type of freezing achieved in these experiments does not mimic the pattern of damage which occurs in the field. Based on mechanisms proposed elsewhere (Lucas, 1954; Proebsting and Andrews, 1982; Anderson and Smith, 1989; Ashworth, 1992), ice nucleation probably initiates at the cane, then propagates through the vascular system of the fruit stem into the top of the fruit. This is consistent with observations from

frost-injured fruit which indicate that inner pericarp tissue adjacent to the point of attachment is the first to freeze. Subsequent damage radiates out towards the surface, and down towards the base of the fruit as the severity of frosting becomes progressively worse (MacRae and Aldridge, 1984; Pyke et al., 1985).

There is much interest in developing real-time NMR techniques for on-line sorting and quality assessment. For example, NMR may be used to evaluate the soluble solids content of fresh prunes (Zion et al., 1995) or determine firmness of tomatoes (Kim et al., 1994). Here we were interested in developing criteria for distinguishing freeze-damaged fruit. Although structural changes, such as deformation and disruption of the seed pattern, may be apparent in the images, it is more difficult to quantify and make assessment decisions based on these characteristics. Quantifiable changes in NMR relaxation parameters or diffusion may consequently prove more useful.

There was a significant decrease in the T_2 relaxation time following freezing-thawing, which can be used to distinguish damaged and undamaged fruit. This can be done with or without imaging. That is, T_2 relaxation changes can be determined spatially at discrete locations within the fruit, or a bulk measurement can be made from the whole fruit. The former takes into account the localised nature of injury in this crop; the latter is advantageous in that it reduces the sophistication of the NMR equipment required, and reduces measurement times. Diffusion was also more rapid in freeze-thawed samples, however, the limitation of the extra hardware required to generate strong diffusion gradients suggests T_2 would be the preferred measurement to exploit in non-destructive applications detecting frost injury.

The specific causes contributing to the changes following freezing observed here are unknown. The spectral analysis (Fig. 5) implies that there is minimal difference between the solution properties of fresh and frozen-thawed fruit, and consequently, that the changes are related to other factors. Duce et al. (1992) and Gamble (1994) have noted decreased image contrast and changes in relaxation following freezing of courgette and blueberry. Using a CPMG pulse sequence, McCarthy et al. (1995) measured a decrease in T_2 in bruised regions of apples. By comparison with gradient-recalled-echo images, they showed that this was attributable to a change in diamagnetic susceptibility due to leakage of fluids into the intercellular air pockets following cellular destruction. This is likely to be a less important mechanism here, since the intercellular gas spaces occupy a much smaller proportion of the fruit volume (2%) relative to apple (20%) (Hallett et al., 1992). Alternatively, relaxation may be affected by the presence of surface 'sinks' (Chui et al., 1995). These are particularly important when the volume in which nuclear spins are free to move in is small compared with the area of surfaces. After cell dehydration and rupture, water is no longer confined to the cell, thus the effect of cell surfaces on relaxation is diminished. Our experiments also showed that diffusion is more rapid in the freeze-thawed samples. Once cell membranes or cells rupture, molecules are less impeded by reflection and adsorption at these barriers. According to the analysis of Tanner (1978), the self-diffusion coefficient of water would be expected to be greater in a situation where effects restricting diffusion were removed.

In summary, NMR imaging has been able to distinguish between freeze-damaged and unaffected tissues in a commercially important fruit crop. Furthermore, there were quantitative differences between the T_2 relaxation, and diffusion properties of these two

types of tissue. These differences may be important in future considerations for designs for on-line sensors assessing fruit quality. Because of differences in the nature of damage sustained by kiwifruit under field- as opposed to experimental-conditions, however, the implications of the spatial nature of freezing effects in kiwifruit will need to be taken into account.

Acknowledgements

This work was funded under a NZ Foundation for Research, Science and Technology Grant (94-HRT-07-406), and a United States Department of Agriculture Award (93-37500-9254). The GE-NMR Omega instrument was partly funded by grants from the National Institute of Health (RR02511) and the National Science Foundation (PCM8417289).

References

Anderson, J.A., Smith, M.W., 1989. Ice propagation in peach shoots and flowers. HortScience 24, 480–482.

Ashworth, E.N., 1992. Formation and spread of ice in plant tissues. Hortic. Rev. 13, 215–255.

Ballagh, K.C., Barnes, T.H., Bittar, A., Ellis, P.J., Hamlin, J.D., Ireland, W., Mason, R.S., Smith, G.J., 1984. Frost damage in kiwifruit examined by non-destructive physical methods. Physics and Engineering Laboratory Report No. 889 (ISSN-0111-2171), Department of Scientific and Industrial Research, Wellington, 25 pp.

Beever, D.J., Hopkirk, G., 1990. Fruit development and fruit physiology. In: Warrington, I.J., Weston, G.C. (Eds.), Kiwifruit: Science and Management. Ray Richards Publishing and N.Z. Society for Horticultural Science, Auckland, pp. 97–126.

Callaghan, P.T., 1991. Principles of Nuclear Magnetic Resonance Microscopy. Clarendon Press, Oxford, 492 pp.

Chen, P., McCarthy, M.J., Kim, S.M., Zion, B., 1995. Development of a high-speed NMR technique for sensing fruit quality. Paper No. 95-3613. ASAE Conference, Chicago, IL.

Chui, M.M., Phillips, R.J., McCarthy, M.J., 1995. Measurement of the porous microstructure of hydrogels by nuclear magnetic resonance. J. Colloid Interface Sci. 174, 336–344.

Duce, S.L., Carpenter, T.A., Hall, L.D., 1992. Nuclear magnetic resonance imaging of fresh and frozen courgettes. J. Food Eng. 16, 165–172.

Edelstein, W.A., Hutchison, J.M.S., Johnson, G., Redpath, T., 1980. Spin warp NMR imaging and applications to human whole-body imaging. Phys. Med. Biol. 25, 751–756.

Gamble, G.R., 1994. Non-invasive determination of freezing effects in blueberry fruit tissue by magnetic resonance imaging. J. Food Sci. 59, 571–573, 610.

Haase, A., Frahm, J., Matthaei, D., Hänicke, W., Merboldt, K.D., 1986. FLASH imaging. Rapid NMR imaging using low flip-angle pulses. J. Magn. Reson. 67, 258–266.

Hallett, I.C., MacRae, E.A., Wegrzyn, T.F., 1992. Changes in kiwifruit cell wall ultrastructure and cell packing during postharvest ripening. Int. J. Plant Sci. 153, 49–60.

Kerr, W.L., Kauten, R.J., Ozilgen, M., McCarthy, M.J., Reid, D.S., 1996. NMR imaging, calorimetric, and mathematical modelling studies of food freezing. J. Food Process Eng., 19: 363–384.

Kim, S.M., McCarthy, M.J., Chen, P., 1994. Feasibility of tomato quality grading and sorting using magnetic resonance. Paper No. 94-6519. ASAE Conference, Atlanta, GA.

Lucas, J.W., 1954. Subcooling and ice nucleation in lemons. Plant Physiol. 29, 245–251.

MacRae, E.A., Aldridge, T., 1984. An assessment of frost damage in kiwifruit. Department of Scientific and Industrial Research Internal Report, Auckland, 46 pp.

McCarthy, M.J., 1994. Magnetic Resonance Imaging in Foods. Chapman and Hall, New York, 110 pp.
McCarthy, M.J., Zion, B., Chen, P., Ablett, S., Darke, A.H., Lillford, P.J., 1995. Diamagnetic susceptibility changes in apple tissue after bruising. J. Sci. Food Agric. 67, 13–20.
Proebsting, E.L., Andrews, P.K., 1982. Supercooling young developing fruit and floral buds in deciduous orchards. HortScience 17, 67–68.
Pyke, N., MacRae, E.A., Hogg, M.G., Stanley, C.J., 1985. Frost damage in many growing areas. N.Z. Kiwifruit, February, p. 16.
Tanner, J.E., 1978. Transient diffusion in a system partitioned by permeable barriers. Application of NMR measurements with a pulsed field gradient. J. Chem. Phys. 69, 1748–1754.
Testolin, R., Costa, G., 1995. Ice nucleation temperatures in kiwifruit. Scientia Hortic. 61, 29–36.
Young, J.M., 1987. Ice-nucleation on kiwifruit. Ann. Appl. Biol. 111, 697–704.
Zion, B., Chen, P., McCarthy, M.J., 1995. Non-destructive quality evaluation of fresh prunes by NMR spectroscopy. J. Sci. Food Agric. 67, 423–429.